Structural, Magnetic, and Electrochemical Properties of Dinuclear Triple Helices: Comparison with Their Mononuclear Analogues

Loïc J. Charbonnière, Alan F. Williams,* Claude Piguet, Gérald Bernardinelli, and Elisabeth Rivara-Minten

Dedicated to Dr. Alfred Maddock on the occasion of his 80th birthday

Abstract: A series of dinuclear triple-helical complexes of iron(II) and cobalt(III) with bis[2-(pyrid-2′-yl)benzimidazol-5-yl]methane ligands **2** were compared with the analogous mononuclear complexes of Fe(II) and Co(III) with 2-(pyrid-2′-yl)benzimidazole ligands **1**. With the dinucleating ligands **2** only one complex is formed, in contrast to the mononuclear complexes, for which stepwise formation is observed. The crystal structures of *fac*-$[Co(\mathbf{1a})_3](ClO_4)_3 \cdot EtCN$ and $[Fe_2(\mathbf{2c})_3](ClO_4)_4 \cdot 4\,CH_3CN$ are reported and compared with previously determined triple-helix structures to show that the formation of the helicate does not involve significant distortion of the metal coordination sphere, and that a decrease in metal–nitrogen bond length results in a longer metal–metal distance. Magnetic susceptibilities were measured between 243 and 323 K in CD_3CN solution for $[Co(\mathbf{1a})_3]^{2+}$, $[Co_2(\mathbf{2a})_3]^{4+}$, $[Fe(\mathbf{1b})_3]^{2+}$, $[Fe_2(\mathbf{2b})_3]^{4+}$, $[Fe(\mathbf{1a})_3]^{2+}$ and $[Fe_2(\mathbf{2a})_3]^{4+}$. Cobalt(II) complexes and iron(II) complexes with methyl substituents at the 6-position of the pyridine rings are high spin and show Curie paramagnetism with no significant metal–metal interaction. Complexes $[Fe_2(\mathbf{2a})_3]^{4+}$ and $[Fe(\mathbf{1a})_3]^{2+}$ are spin-crossover systems; the dinuclear complex shows greater stability in the low-spin form. Electrochemistry does not allow the separation of the two oxidation waves of $[M_2(\mathbf{2a})_3]^{4+}$, but the ^1H NMR spectrum of $[Co^{II}Co^{III}(\mathbf{2a})_3]^{5+}$ shows the system to be a class II mixed-valent system. The oxidation of the metal ions is not a cooperative phenomenon.

Keywords: helical structures · magnetic properties · mixed-valent compounds · N ligands · spin crossover

Introduction

The synthesis of helical coordination complexes (helicates) has attracted considerable attention lately and has been the subject of a number of recent reviews.[1–3] The rapid self-assembly of these sophisticated structures[4] is typical of supramolecular chemistry.[5] The modification of both the ligands and the metal ions is straightforward and has provided insights into the relative importance of different factors in the assembly process. Among the properties of the resulting helical complexes, the chirality,[6–8] electrochemistry,[9–11] and energy transfer[12,13] have been studied. We have previously studied a series of triple-helix complexes in which two octahedral metal ions are complexed by three bis-bidentate ligands of type **2** (Scheme 1).[14] Surprisingly, racemization of the enantiomerically pure triple helix (+)-$[Co_2(\mathbf{2a})_3]^{4+}$ was very slow at room temperature[15] relative to the isomerization of the analogous mononuclear complex $[Co(\mathbf{1a})_3]^{2+}$.[16] Further studies showed the origin of this inertness to be the rigidity of the helical system, the reorganization of the coordination sphere of one metal being impossible without perturbing the coordination sphere of the other.

This observation raises the general question of the extent to which the incorporation of a metal ion into a dinuclear helical structure modifies its properties relative to a simple mononuclear complex. Both electronic effects arising from the relative proximity of the two metal ions and their interaction, and mechanical effects due to the linking of two metal ions by a relatively rigid binucleating ligand can be envisaged. The inertness of the triple helix $[Co_2(\mathbf{2a})_3]^{4+}$ is an example of a mechanical effect. A more subtle effect is seen in $[Co_2(\mathbf{2b})_3]^{4+}$, in which the methyl substituents at the 6-position of the pyridyl moieties limit the approach of the pyridine rings to the metal ion and thus influence the redox potential of the cobalt ion;[10] in this case the helical architecture is important in that

[*] Prof. A. F. Williams, Dr. L. J. Charbonnière, Dr. C. Piguet, Dr. E. Rivara-Minten
Département de Chimie Minérale, Analytique et Appliquée
Universite de Genève
30 quai Ernest Ansermet, CH-1211 Genève 4 (Switzerland)
Fax: (+ 41) 22-702-6069.
E-mail: alan.williams@§chiam.unige.ch
Dr. G. Bernardinelli
Laboratoire de Cristallographie aux Rayons-X
Université de Genève (Switzerland)

  0947-6539/98/0403-0485 $ 17.50+.25/0

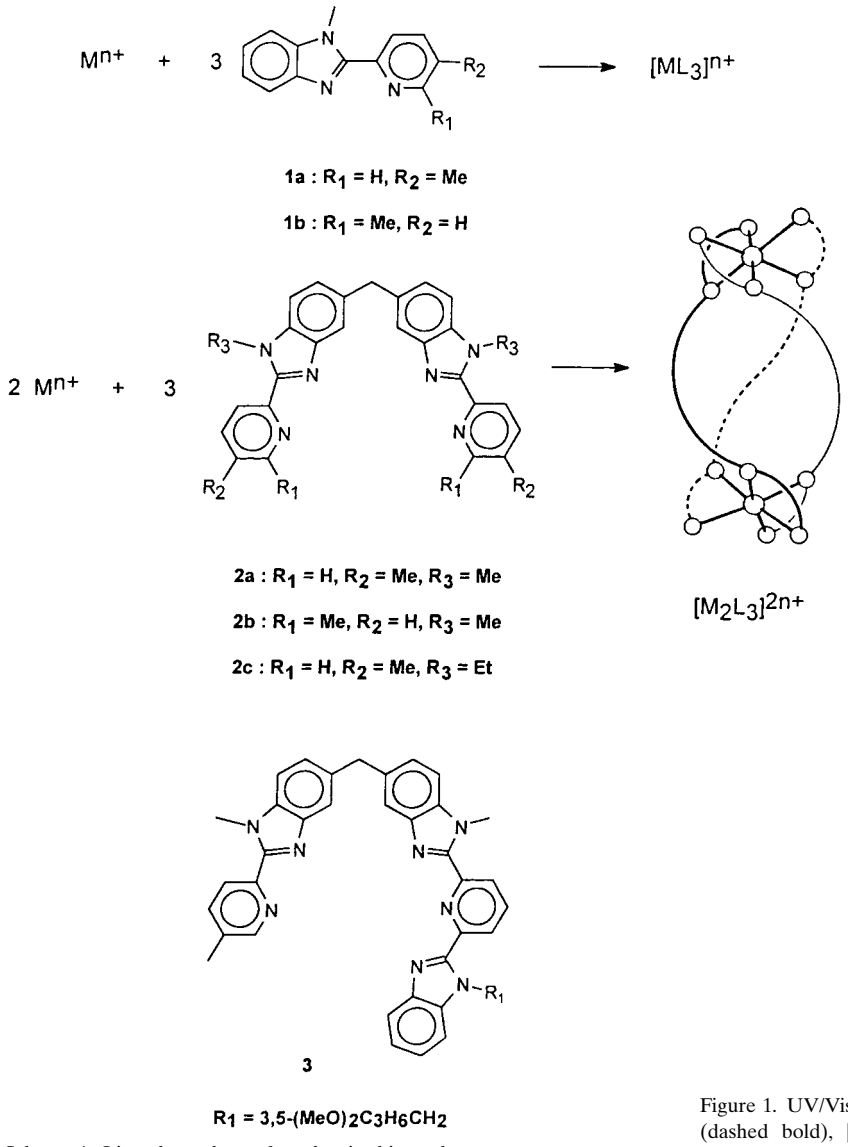

Scheme 1. Ligands used or referred to in this work.

it holds the three interacting methyl groups on the same face of the coordination octahedron.

Here we report on the structure, magnetism and redox properties of the triple helices, with a view to evaluating the importance of electronic and mechanical interactions. As in isomerization studies,[16,17] the properties of the dinuclear triple-helix complexes of **2** are compared with those of analogous mononuclear complexes of **1**.

Results

Synthesis and characterization of complexes: The complexes $[FeL_3]^{2+}$ (L = **1a, 1b**) and $[Fe_2L_3]^{4+}$ (L = **2a, 2b, 2c**) were isolated as crystalline perchlorate salts. The IR spectra showed bands due to coordinated ligands and free perchlorate ions, and the ESMS spectra showed the expected peaks for $[Fe(\mathbf{1})_3]^{2+}$ and $[Fe_2(\mathbf{2})_3]^{4+}$. The dinuclear species also showed peaks due to $[Fe_2(\mathbf{2})_3(ClO_4)_x]^{(4-x)+}$ cations ($x = 1,2$). The UV/Vis spectra in acetonitrile (Figure 1) showed an intense band in the region 300–340 nm assigned to $\pi \rightarrow \pi^*$ transitions of the ligand. The complexes $[Fe(\mathbf{1a})_3]^{2+}$, $[Fe_2(\mathbf{2a})_3]^{4+}$ and $[Fe_2(\mathbf{2c})_3]^{4+}$ showed metal-to-ligand charge-transfer (MLCT) bands typical of low-spin Fe^{II}[18–20] in the region 520–530 nm, which are responsible for their violet colour. Complexes $[Fe(\mathbf{1b})_3]^{2+}$ and $[Fe_2(\mathbf{2b})_3]^{4+}$ are yellow and do not show the charge transfer band, although $[Fe(\mathbf{1b})_3]^{2+}$ showed a weak shoulder at 385 nm ($\varepsilon = 972\ M^{-1}cm^{-1}$) which may be due to a MLCT transition that is shifted to higher energy in a high-spin complex.

The distinction between high- and low-spin complexes suggested by the UV/Vis spectra was confirmed by the ^1H NMR spectra in CD_3CN. The high-spin complexes $[Fe(\mathbf{1b})_3]^{2+}$ and $[Fe_2(\mathbf{2b})_3]^{4+}$ showed only very broad peaks, while low-spin $[Fe_2(\mathbf{2a})_3]^{4+}$ and $[Fe_2(\mathbf{2c})_3]^{4+}$ showed the spectra expected for a diamagnetic D_3 symmetric species, although the signals were slightly broadened by the presence of traces of high-spin iron(II). Figure 2 shows the ^1H NMR spectrum of $[Fe_2(\mathbf{2c})_3]^{4+}$, and Scheme 2

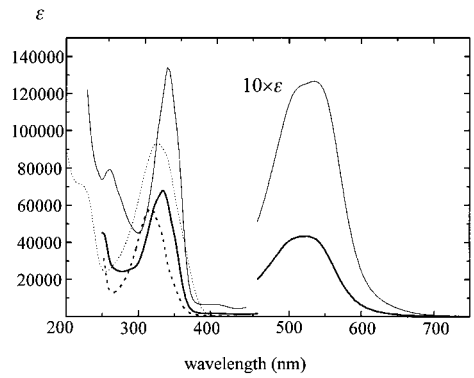

Figure 1. UV/Vis spectra of $[Fe(\mathbf{1a})_3]^{2+}$ (unbroken bold), $[Fe(\mathbf{1b})_3]^{2+}$ (dashed bold), $[Fe_2(\mathbf{2a})_3]^{4+}$ (unbroken), and $[Fe_2(\mathbf{2b})_3]^{4+}$ (dashed) in acetonitrile at 22 °C.

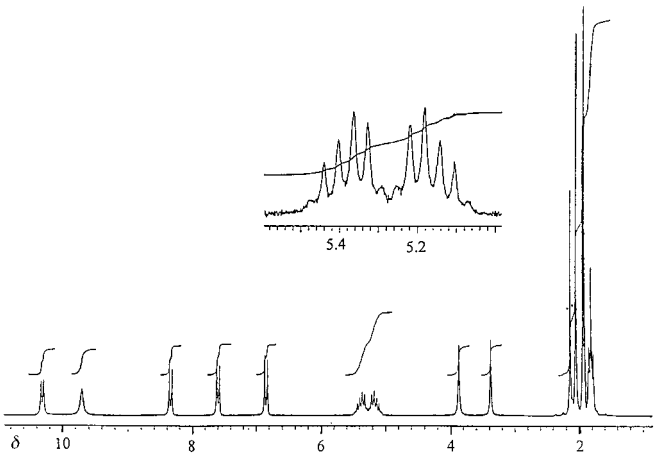

Figure 2. ^1H NMR spectrum of $[Fe_2(\mathbf{2c})_3]^{4+}$ in CD_3CN at 22 °C.

0947-6539/98/0403-0486 $ 17.50+.50/0 Chem. Eur. J. 1998, 4, No. 3

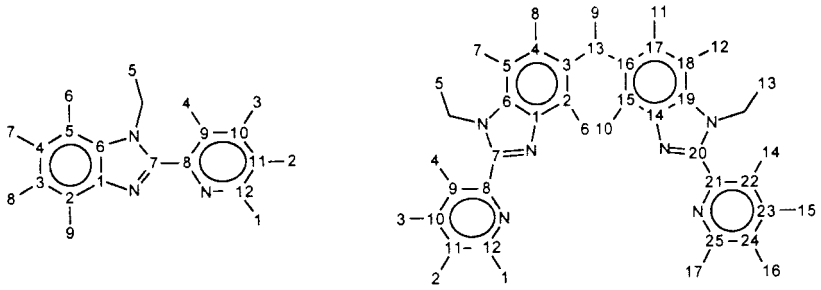

Scheme 2. Numbering scheme for carbon and hydrogen atoms.

the atom numbering. The helical nature of the complex is clearly shown by the ABX_3 spin system of the ethyl groups, which gives rise to a multiplet around $\delta = 5.30$. The ^1H NMR spectrum of $[Fe(\mathbf{1a})_3]^{2+}$ at room temperature is composed of broad peaks, poorly resolved and spread over a few tens of ppm. This behaviour is attributed to the presence of both *fac* and *mer* isomers and to a large fraction of high-spin Fe^{II} (vide infra). Changing the solvent ($[D_6]$acetone) or lowering the temperature (243 K) did not improve the spectrum.

The complex $[Co(\mathbf{1a})_3](ClO_4)_3$ was obtained by oxidation of $[Co(\mathbf{1a})_3](ClO_4)_2$[16] in acetonitrile with $H_2O_2/HClO_4$ and a catalytic amount of $[Cp_2Fe](BF_4)$. The ^1H NMR spectrum of the isolated salt shows 36 signals in the range $\delta = 0-10$, and this indicates a mixture of *fac* and *mer* isomers of the low-spin cobalt(III) complex. On oxidation, the *mer*/*fac* ratio changed from 82/18 for Co^{II} to 64/36 for Co^{III}. The inert Co^{III} complexes were separated on a cation-exchange resin with HCl as eluent. Evaporation of the acid after elution allowed the recovery of the pure isomers but in very low yields, probably as a result of partial decomposition in the acidic medium. The purity of the isomers was verified by ^1H NMR spectroscopy, which showed nine signals for the *fac* isomer and 27 for the *mer* isomer. COSY and NOEDiff experiments allowed assignment of all peaks, including the 27 different protons of the *mer* isomer. The *fac* isomer was eluted second and was isolated as X-ray quality crystals of the perchlorate salt by recrystallization from propionitrile/*tert*-butyl methyl ether.

A notable difference between ligands **1** and **2** was observed upon titrating the free ligand with M^{II} salts. With **1** both Co^{II} and Fe^{II} showed stepwise formation of complexes, whereas with the binucleating ligands **2** only $[M_2L_3]^{4+}$ was observed; the UV/Vis spectra showed isosbestic points. This was confirmed by factor analysis of the spectroscopic titration data, followed by least-squares fitting of the equilibria for ligands **1** [Eqs. (1–3)]. For ligands **2** the equilibrium of Equation (4) was fitted. The stability constants are listed in Table 1.

$$M^{2+} + L \rightleftharpoons [ML]^{2+} \quad (1)$$

$$[ML]^{2+} + L \rightleftharpoons [ML_2]^{2+} \quad (2)$$

$$[ML_2]^{2+} + L \rightleftharpoons [ML_3]^{2+} \quad (3)$$

$$2M^{II} + 3L \rightleftharpoons [M_2L_3]^{4+} \quad (4)$$

Table 1. Stability constants for complexes measured at 22 °C in acetonitrile.

Metal	Ligand	$\log\beta_1$	$\log\beta_2$	$\log\beta_3$	$\log\beta_{23}$	
Fe^{II}	**1a**	6.4(2)	12.2(3)	17.6(3)		
Fe^{II}	**1b**	6.1(3)	11.0(4)	15.2(4)		
Co^{II}	**1a**	7.8(1)	14.9(2)	21.2(3)		ref. [16]
Fe^{II}	**2a**				19.6(8)	
Fe^{II}	**2b**				22.6(6)	
Fe^{II}	**2a**				20.2(2)	
Co^{II}	**2a**				> 25	ref. [10]
Co^{II}	**2b**				21.9(2)	ref. [10]

Structural analysis:

*Crystal structure of fac-[Co(**1a**)$_3$](ClO$_4$)$_3$·EtCN*: The crystal structure of the complex shows a $[Co(\mathbf{1a})_3]^{3+}$ cation with three non-coordinated perchlorate anions and a slightly disordered propionitrile molecule. The unit cell contains two cations with opposite absolute configurations, and the crystal structure exhibits alternating planes in which the cations all have the Δ or Λ configuration. The pyridine and benzimidazole rings are planar within experimental error. No particular intermolecular interactions were observed. The cation is composed of three **1a** ligands coordinated to the Co^{III} atom in a *fac* arrangement; a pseudo-C_3 axis passing through the cobalt centre relates the three ligands. The coordination sphere around Co^{III} is a pseudooctahedron flattened along the pseudo-C_3 axis, as reported for $[Co(bipy)_3]^{3+}$.[21] The average $Co-N_{py}$ distance is 1.96(1) Å, 0.03 Å longer than in $[Co(bipy)_3]^{3+}$ and close to that in $[Co_2(\mathbf{2a})_3]^{6+}$,[8] as is the average $Co-N_{Bz}$ distance of 1.91(1) Å. The average dihedral angle between pyridine and benzimidazole rings on the same ligand is 2.2°, and the average bite angle N_{py}-Co^{III}-N_{Bz} is 82.2°. A stereoscopic view of the Δ-*fac*-$[Co(\mathbf{1a})_3]^{3+}$ cation is shown in Figure 3.

*Crystal structure of [Fe$_2$(**2c**)$_3$](ClO$_4$)$_4$·4CH$_3$CN*: The crystal structure contains a $[Fe_2(\mathbf{2c})_3]^{4+}$ cation, noncoordinated perchlorate anions and acetonitrile molecules in large interstices between the helices. The cation is a dinuclear triple helix

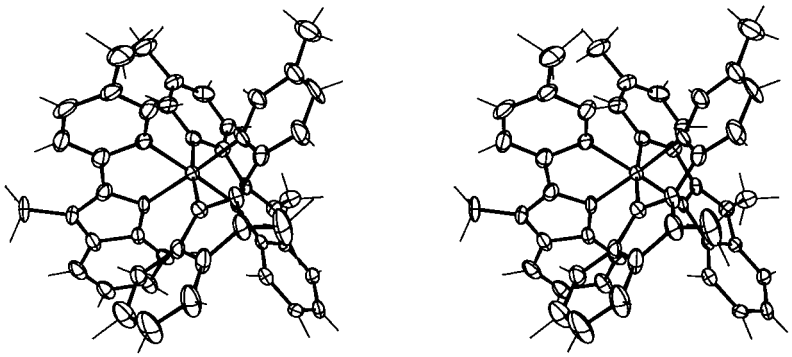

Figure 3. ORTEP[48] stereoview of the *fac*-$[Co(\mathbf{1a})_3]^{3+}$ cation. Ellipsoids are shown at the 50% probability level.

(Figure 4) in which the three ligands are wrapped around a pseudo-C_3 axis passing through the two iron atoms. It is situated on a crystallographic C_2 axis that passes through the C13 bridge of one ligand. No stacking between aromatic groups was observed, and the structure shows no significant intermolecular interactions. The pyridine and benzimidazole groups are planar within experimental error. Helicity results from rotation about the interannular C–C bonds of the ligands, as observed previously for analogous helical complexes.[1–3,22] The unit cell contains four cations, two with Δ and two with Λ chirality. The coordination sphere around the Fe(II) centre is a pseudooctahedron slightly flattened along the pseudo-C_3 axis. The average Fe–N distances are Fe–N_{py} 2.00(2) and Fe–N_{Bz} 1.96(1) Å, typical for low-spin Fe^{II} coordinated to imine nitrogen atoms.[23] The average bite angle N_{py}-Fe-N_{Bz} is 80.8(7)°, almost identical to that found by Elliott et al. (81.2°).[9b] The Fe–Fe distance is 9.163(5) Å.

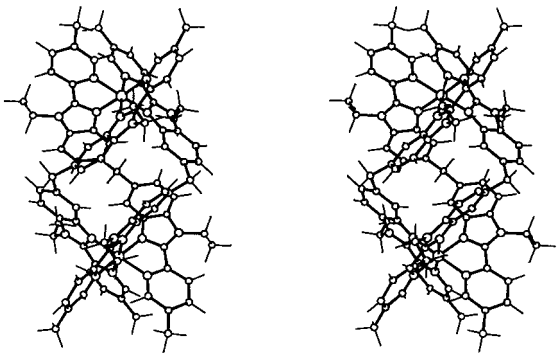

Figure 4. ORTEP[48] stereoview of the $[Fe_2(\mathbf{2c})_3]^{4+}$ cation.

Comparison of the structures: The two structures described above, together with those published previously for the cations $[Co_2(\mathbf{2a})_3]^{4+}$, $[Co_2(\mathbf{2b})_3]^{4+}$,[10] and $[Co_2(\mathbf{2a})_3]^{6+}$,[8] allow the structural differences resulting from a change of metal ion or from introducing steric repulsion into the ligand (e.g., **2b**) to be analyzed. To discuss the geometry of the coordination sphere, we regard the pseudooctahedron as being formed from two tripods with C_3 symmetry (Scheme 3), one formed by M–N_{py} bonds, and the other by M–N_{Bz} bonds.[10] The coordination sphere can then be discussed in terms of the M–N distances, the bite angle of the chelates, the dihedral angle χ of the bond joining the benzimidazole and pyridine groups of the chelates, the flattening angles θ of the tripods, which represent the extent to which the octahedron has been deformed along the C_3 axis (for an ideal octahedron $\theta = 54.7°$) and the twist angle ω, which measures the extent to which one tripod has been rotated about the threefold axis relative to the other ($\omega = 60°$ for a perfect octahedron, 0° for a trigonal prism).

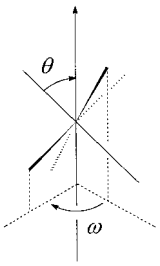

Scheme 3. The coordination octahedron is regarded as two C_3 tripods sharing a common apex. θ is the flattening angle, and ω is the twist angle indicating the extent to which the lower tripod is rotated with respect to the upper.

The relative orientation of the two bidentate domains of ligand **2** can be characterized by the torsion angles C2-C3-C13-C16 and C3-C13-C16-C15 (Schemes 2 and 4). When these angles are zero, the two bidentate domains are closest to each other; as the torsion increases they move apart and reach a maximum separation for torsion angles of 180°. The three pseudo-C_2 axes of the pseudo-D_3 helicates require these two torsion angles to be equal in an ideal structure. The second parameter used to characterize the overall structure of the complex is the area S_{C13} of the triangle formed by the three hinge methylene carbon atoms C13 joining the benzimidazole moieties. Large values of S_{C13} imply that the helix is flattened along the axis, and small values correspond to elongation along the axis, which brings the ligand strands closer together. Table 2 lists the values of these parameters, averaged under the assumption of D_3 symmetry for the triple helicates and C_3 symmetry for $[Co(\mathbf{1a})_3]^{3+}$. Since the ^{1}H NMR spectra show clearly that the complexes have D_3 symmetry in solution, this averaging is reasonable.

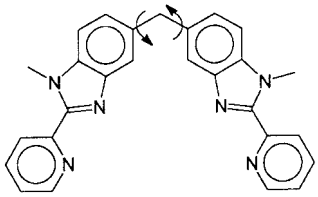

Scheme 4. The two torsion angles used to characterize the opening of the ligand **2**.

The data in Table 2 show that the coordination sphere in $[Co_2(\mathbf{2a})_3]^{6+}$ is identical within experimental error to that of *fac*-$[Co(\mathbf{1a})_3]^{3+}$; clearly the formation of the dinuclear triple helix does not impose any strain upon the coordination sphere of the metal ion. This would seem to be generally true for the other complexes, since the metal–nitrogen distances agree well with those reported for nonhelical complexes,[23] with the exception of $[Co_2(\mathbf{2b})_3]^{4+}$, in which the methyl substituents of the pyridine rings are known to repel each other.[10] The decrease in the bite angle on crossing the series is a reflection of the increase in metal–nitrogen bond length.

The metal–metal distances in these complexes show considerable variation, and it is interesting to correlate them with the structural parameters of the helix. Imagine a triple-helical complex $[M_2(\mathbf{2})_3]^{2n+}$ in which the M–N distance is

Table 2. Averaged structural parameters for triple helical complexes and *fac*-$[Co(\mathbf{1a})_3]^{3+}$.

Parameter	*fac*-$[Co(\mathbf{1a})_3]^{3+}$	$[Co_2(\mathbf{2a})_3]^{6+}$	$[Fe_2(\mathbf{2c})_3]^{4+}$	$[Co_2(\mathbf{2a})_3]^{4+}$	$[Co_2(\mathbf{2b})_3]^{4+}$
$d_{M-N(bzim)}$ (Å)	1.912(9)	1.92(3)	1.96(3)	2.11(3)	2.06(2)
$d_{M-N(py)}$ (Å)	1.953(12)	1.96(3)	2.00(1)	2.17(3)	2.29(6)
average d_{M-N} (Å)	1.93(3)	1.94(3)	1.98(3)	2.14(4)	2.18(12)
bite angle (°)	82.2(2)	83.1(2)	80.8(6)	76.6(9)	76.2(16)
dihedral angle χ (°) [a]	1(3)	2(4)	3(3)	9(9)	20(5)
θ (°)	58.4(17)	57.8(14)	58.8(7)	60.2(20)	62(4)
ω (°)	55.7(17)	55.7(15)	54.2(5)	50.5(15)	54.6(12)
torsion (°)[b]		55(2)	56(2)	53(4)	47(7)
S_{C13} (Å^2)		22.5(10)	22.4(10)	23.9(10)	26.8(10)
d_{M-M} (Å)		9.146(6)	9.163(5)	8.854(4)	8.427(4)
Ref.		[8]		[10]	[10]

[a] The average torsion angle of the N-C-C-N fragment of the chelate ring. [b] The torsion angles averaged are C2-C3-C13-C16 and C3-C13-C16-C15.

0947-6539/98/0403-0488 $ 17.50+.50/0 *Chem. Eur. J.* **1998**, *4*, No. 3

suddenly shortened (for example, by oxidation or a high- to low-spin transition). The bidentate domain will try to move closer to the helical axis, and examination of a model shows two ways in which it can do this: reduction of the C3-C13-C16 bond angle or an increase in the torsion angles C2-C3-C13-C16 and C3-C13-C16-C15. We would expect the change in the torsion angle to be less expensive energetically, and indeed the C3-C13-C16 bond angles show no significant variation in these structures. The torsion angles show a considerable spread, but the average for assumed D_3 symmetry shows the expected increase as the bidentate domains move further apart and the metal–metal distance increases. Similarly, C13 moves closer to the helical axis, and this leads to a decrease in S_{C13}. A further prediction of the model is that the flattening angle θ should decrease, as should the twist angle ω, but these angles are equally modified directly by a decrease in metal–nitrogen bond length, which leads to an increase in θ and a decrease in ω. It is difficult to ascertain the relative importance of each effect in the changes in these parameters. It does, however, seem clear that the metal–nitrogen distance can influence the pitch of the helix and therefore the metal–metal distance.

Magnetic properties of the complexes: The molar susceptibilities and effective magnetic moments of complexes $[Co(\mathbf{1a})_3]^{2+}$, $[Co_2(\mathbf{2a})_3]^{4+}$, $[Fe(\mathbf{1b})_3]^{2+}$, $[Fe_2(\mathbf{2b})_3]^{4+}$, $[Fe(\mathbf{1a})_3]^{2+}$ and $[Fe_2(\mathbf{2a})_3]^{4+}$ were measured in CD_3CN between 240 and 330 K by the Evans method,[24] adapted for large diamagnetic contributions.[25]

Co^{II} complexes: The molar magnetic susceptibility of $[Co(\mathbf{1a})_3]^{2+}$ followed a Curie–Weiss law ($\chi = C/(T-\theta)$), where $C = 2.9(3)\ cm^3 mol^{-1} K^{-1}$ and $\theta = 2(3)$ K. The small value of θ suggests essentially Curie-type behaviour for this cobalt complex, and the effective magnetic moment was constant, with an average value of 4.85 BM, typical of high-spin Co^{II} complexes.[26] The dinuclear Co^{II} triple helix $[Co_2(\mathbf{2a})_3]^{4+}$ also showed Curie-type behaviour, with $C = 6.2(1)\ cm^3 mol^{-1} K^{-1}$ ($\theta = -1(6)$ K for a Curie–Weiss fit). The effective magnetic moment was constant, with an average value of 7.03 BM. If the two metals in the helix are magnetically independent, the magnetic susceptibility of the complex would be expected to be the sum of the susceptibilities of two mononuclear subunits equivalent to *fac*-$[Co(\mathbf{1a})_3]^{2+}$. The observed value of $6.2(1)\ cm^3 mol^{-1} K^{-1}$ is indeed very close to twice that observed for $[Co(\mathbf{1a})_3]^{2+}$, and the slight difference may be due to the fact that in solution $[Co(\mathbf{1a})_3]^{2+}$ is a 82/18 mixture[16] of *mer* and *fac* isomers. These results indicate that the magnetic coupling between the two cobalt ions is negligible in the triple helix, as expected from the large intermetallic distance of 8.855 Å. The value of θ close to zero is also consistent with two magnetically independent nuclei with no significant interaction.

Fe^{II} complexes: The molar magnetic susceptibility of $[Fe(\mathbf{1b})_3]^{2+}$ (Figure 5) showed a slight deviation from Curie-type behaviour, with $C = 3.7(1)\ cm^3 mol^{-1} K^{-1}$ and $\theta = -10(3)$ K. The nonzero value of θ may arise from changes in the *mer/fac* ratio with temperature,[27] although this was not

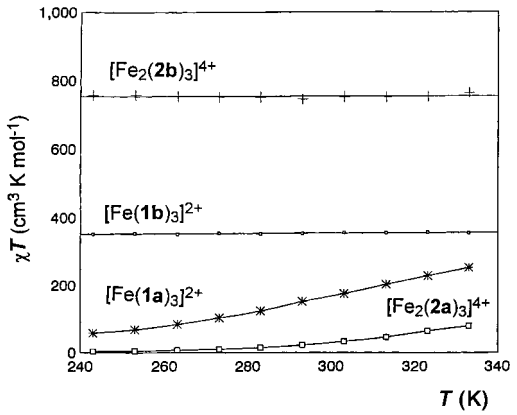

Figure 5. χT as a function of T for $[Fe(\mathbf{1a})_3]^{2+}$, $[Fe(\mathbf{1b})_3]^{2+}$, $[Fe_2(\mathbf{2a})_3]^{4+}$ and $[Fe_2(\mathbf{2b})_3]^{4+}$ in acetonitrile.

seen for $[Co(\mathbf{1a})_3]^{2+}$.[16] The effective magnetic moment was constant, with an average value of 5.24 BM, typical of high-spin Fe^{II} complexes.[26] The magnetic susceptibility of the dinuclear triple helix $[Fe_2(\mathbf{2b})_3]^{4+}$ followed Curie-type behaviour with $C = 7.4(1)\ cm^3 mol^{-1} K^{-1}$ (a Curie–Weiss fit gave $\theta = -3(4)$ K). As for $[Co_2(\mathbf{2a})_3]^{4+}$, C was twice that of the mononuclear analogue, indicating a negligible magnetic coupling of the two nuclei in the triple helix. The effective magnetic moment is constant, with a mean value of 7.65 BM.

For $[Fe(\mathbf{1a})_3]^{2+}$ the magnetic susceptibility shows non-Curie behaviour, the effective magnetic moment increasing with temperature (Figure 5) as a result of a spin-crossover transition from the low-spin $^1A_1$ to the high-spin $^5T_2$ electronic state in pseudo-O_h symmetry [Eq. (5)], which is well known

$$^1A_1 \overset{K_{sc}}{\rightleftharpoons} {}^5T_2 \qquad (5)$$

for Fe^{II} complexes having polyimine-type ligands.[28] The transition is described by the equilibrium constant K_{sc}, which is the ratio between the molar fractions of the high- and low-spin configurations and may be obtained from Equation (6).[19] Here x_{HS} and x_{LS} are the molar fractions of high-

$$K_{sc} = \frac{x_{HS}}{x_{LS}} = \frac{x_{HS}}{1 - x_{HS}} = \frac{\chi_{obs} - \chi_{HS}}{\chi_{LS} - \chi_{obs}} = \frac{\mu_{eff}^2 - \mu_{LS}^2}{\mu_{HS}^2 - \mu_{eff}^2} \qquad (6)$$

and low-spin Fe^{II}, χ_{obs} is the observed molar magnetic susceptibility, χ_{HS} and χ_{LS} are the susceptibilities for completely high-spin and low-spin complexes, μ_{eff} is the effective magnetic moment and μ_{HS} and μ_{LS} are the effective magnetic moments for pure high-spin and low-spin complexes. By taking $\mu_{LS} = 0$, and $\mu_{HS} = 5.24$ BM from the value for $[Fe(\mathbf{1b})_3]^{2+}$, values for K_{sc} were calculated that led to $\Delta H^0 = 20.1(8)\ kJ mol^{-1}$ and $\Delta S^0 = 67(3)\ mol^{-1} K^{-1}$, typical for this type of complex.[19,28] The transition temperature $T_{1/2}$, for which $x_{HS} = x_{LS} = 0.5$, was 299 K. The plot of $\ln K_{sc}$ against $1/T$ was slightly curved; possible reasons for this deviation are: a) a nonzero value of μ_{LS}, as observed for similar complexes[29] (however, variation of the value in the range 0–0.7 BM did not improve the fit); b) the presence of Fe^{III} impurities, which we discount since this would require more than 10 % Fe^{III}; and c) a change in the *mer/fac* isomer ratio with temperature. This has already been observed for tris(2-methylaminopyridine)-

iron(II) iodide.[27] In the solid state, this complex shows *mer* high-spin and *fac* high-and low-spin isomers, but no *mer* low-spin isomer at room temperature.

For the dinuclear triple helix $[Fe_2(\mathbf{2a})_3]^{4+}$, spin crossover is also observed, but the transition was far from complete, even at the highest temperature. Clearly $[Fe_2(\mathbf{2a})_3]^{4+}$ is stabilized in the low-spin form relative to $[Fe(\mathbf{1a})_3]^{2+}$. Using the values of $\mu_{LS}=0$ and $\mu_{HS}=7.65$ BM one can calculate K_{sc2} for the double spin transition [Eq. (7)].

$$[Fe(LS)_2(\mathbf{2a})_3]^{4+} \overset{K_{sc2}}{\rightleftharpoons} [Fe(HS)_2(\mathbf{2a})_3]^{4+} \quad (7)$$

A plot of $\ln K_{sc}$ against $1/T$ with the values for which $\mu_{eff} > 1$ BM (to avoid large errors from a possible nonzero value of μ_{LS}) gave $\Delta H^0 = 31.1(4)$ kJ mol^{-1} and $\Delta S = 76(3)$ J mol^{-1} K^{-1} and did not show the curvature observed for $[Fe(\mathbf{1a})_3]^{2+}$, which is consistent with this effect arising from a mixture of *mer* and *fac* isomers. These values should be regarded as indicative since a complete crossover was not observed, and it is possible that, in the temperature range studied, the transition takes place only to the mixed-spin species $[Fe(LS)Fe(HS)(\mathbf{2a})_3]^{4+}$.

Electrochemistry and electron-transfer properties: $[Fe(\mathbf{1a})_3]^{2+}$, $[Fe_2(\mathbf{2a})_3]^{4+}$ and $[Fe_2(\mathbf{2c})_3]^{4+}$ had similar cyclic voltammograms, with Fe^{II}/Fe^{III} oxidation waves near $+0.8$ V vs. SCE (Table 3). The peaks were broadened due to the presence of *mer* and *fac* isomers for $[Fe(\mathbf{1a})_3]^{2+}$ and by two

Table 3. Electrochemical data, $E_{1/2}$ (ΔE_p), for complexes as perchlorate salts in acetonitrile (0.1M Bu_4NPF_6). $E_{1/2}$ in V vs SCE; ΔE_p in mV.

Complex	$M^{III} \rightarrow M^{II}$	Ligand reduction	Ref.
$[Fe(\mathbf{1a})_3]^{2+}$	+0.80 (75)	−1.40 (100), −1.58 (90)	
$[Fe_2(\mathbf{2a})_3]^{4+}$	+0.85 (100)	−1.43 (100), −1.69 (110)	
$[Fe_2(\mathbf{2c})_3]^{4+}$	+0.84 (120)	−1.41 (130), −1.71 (85)	
$[Fe(\mathbf{1b})_3]^{2+}$	n.o.[a]	−1.08 irr[a]	
$[Fe_2(\mathbf{2b})_3]^{4+}$	n.o.	−1.48 irr	
$[Co(\mathbf{1a})_3]^{3+}$	+0.44 (90)	−1.17 (110), −1.33 irr	
$[Co_2(\mathbf{2a})_3]^{4+}$	+0.37 (160)	−1.19 (90), −1.68 irr	[10]
$[Co_2(\mathbf{2b})_3]^{4+}$	n.o.	−1.05 (90), −1.25 irr	[10]
$[Co_2(\mathbf{2c})_3]^{4+}$	+0.38 (105)	−1.13 (60), −1.71 irr	

[a] n.o.: not observed; irr: irreversible.

successive one-electron oxidations for $[Fe_2(\mathbf{2a})_3]^{4+}$ and $[Fe_2(\mathbf{2c})_3]^{4+}$.[9] Ligand-centred reduction was observed at potentials below −1.4 V. $[Fe(\mathbf{1b})_3]^{2+}$ and $[Fe_2(\mathbf{2b})_3]^{4+}$ showed no wave corresponding to oxidation of Fe^{II}, and at negative potentials gave a broad, irreversible reduction wave. Successive sweeping of the potential showed the voltammograms to be irreproducible, presumably because of deposition of material on the surface of the electrodes.

The cyclic voltammogram obtained for $[Co_2(\mathbf{2c})_3]^{4+}$ was very similar to that previously found for $[Co_2(\mathbf{2a})_3]^{4+}$.[10] Surprisingly, however, $[Co(\mathbf{1a})_3]^{2+}$ exhibited a Co^{II}/Co^{III} oxidation wave at +0.44 V, significantly higher than the values for $[Co_2(\mathbf{2a})_3]^{4+}$ and $[Co_2(\mathbf{2c})_3]^{4+}$. Note that the *mer*/*fac* ratio decreases from 82/18 for $[Co(\mathbf{1a})_3]^{2+}$[16] to 64/36 for $[Co(\mathbf{1a})_3]^{3+}$, as determined by NMR spectroscopy after oxidation.

Since the cyclic voltammetry experiments gave little information on the stability of the mixed-valent helicates, a synthetic approach was adopted. Equimolar amounts of $[Co_2(\mathbf{2a})_3]^{4+}$ and $[Co_2(\mathbf{2a})_3]^{6+}$ were mixed in CD_3CN and the ^1H NMR spectrum of the solution monitored. Immediately after mixing, the spectrum corresponded to a mixture of the starting materials, but after 30 min a new species with a spectrum showing 17 signals was clearly visible, and this steadily increased to an equilibrium value over one day. The spectrum of the new species could be analysed in terms of eight signals typical of a benzimidazole-pyridine ligand bound to Co^{III}, as in $[Co_2(\mathbf{2a})_3]^{6+}$, and eight signals typical of the ligand bound to a paramagnetic Co^{II} centre. The final signal, assigned to the methylene bridge joining the two halves of the ligand, appeared as a broad AB spin system at $\delta = -0.82$. This spectrum corresponded that expected for a localized mixed-valent complex $[Co_2(\mathbf{2a})_3]^{5+}$ with one paramagnetic and one diamagnetic centre, and the assignment was confirmed by COSY and NOEDiff measurements. The clear separation of the diamagnetic and paramagnetic domains of the complex indicates a class II mixed-valent complex and implies that intramolecular exchange between Co^{II} and Co^{III} centres is slow on the NMR timescale, presumably as a result of the considerable change in Co–N bond lengths and the spin change upon electron transfer.[30,31] The long time required for the establishment of equilibrium [Eq. (8)] is, however, probably a result of the highly unfavourable outer-sphere term associated with the interaction between +4 and +6 ions in acetonitrile in the absence of added electrolyte.

$$[Co^{II}_2(\mathbf{2a})_3]^{4+} + [Co^{III}_2(\mathbf{2a})_3]^{6+} \overset{K_{comp}}{\rightleftharpoons} 2[Co^{II}Co^{III}(\mathbf{2a})_3]^{5+} \quad (8)$$

Integration of the signals of the different complexes allowed the calculation of the comproportionation constant $K_{comp} = 6.5(1)$ in CD_3CN. This is slightly higher than the statistical value of four[32] and implies that the oxidation of one Co^{II} centre does not favour the oxidation of the other and that the process is noncooperative. From K_{comp} one may calculate $\Delta E_{1/2}$, the difference in oxidation potential between the couples $[Co_2(\mathbf{2a})_3]^{4+}/[Co_2(\mathbf{2a})_3]^{5+}$ and $[Co_2(\mathbf{2a})_3]^{5+}/[Co_2(\mathbf{2a})_3]^{6+}$ by Equation (9).[32] This value is in accord with

$$\Delta E_{1/2} = (RT/F)\ln K_{comp} = 46 \text{ mV} \quad (9)$$

the broadening ($\Delta E_p = 105$ mV) observed for the oxidation peak in the cyclic voltammogram of $[Co_2(\mathbf{2a})_3]^{4+}$. Elliott et al.[9] have prepared a series of dinuclear triple helices of Fe^{II} with 4,4′-disubstituted 2,2′-bipyridine ligands in which the length of the spacer can be varied. They have used the electrochemically determined values of $\Delta E_{1/2}$ and the intermetallic distances r from X-ray crystallography or molecular modelling calculations to calculate ε, the dielectric constant of the medium. The values for ε lie between 12.3, the value for pyridine, and 39, the value for the solvent acetonitrile. For $[Co_2(\mathbf{2a})_3]^{5+}$, with an estimated value of r as the average of the isovalent Co^{II} and Co^{III} helices, 9.00 Å, we obtain a value for ε of 34.7.

0947-6539/98/0403-0490 $ 17.50+.50/0 *Chem. Eur. J.* **1998**, *4*, No. 3

Discussion

We now return to the question raised in the introduction concerning the nature of the differences between mono- and dinuclear species. Clearly, in the systems studied here the electronic interactions are weak, as shown by the magnetic behaviour of the high-spin systems, by the single metal-centred oxidation or reduction peak observed electrochemically, and the value of the comproportionation constant K_{comp} of 6.5(1) for $[Co_2(\mathbf{2a})_3]^{5+}$, which is close to the statistical value of four. Given the relatively long metal–metal distances, this is not unexpected. Mechanical interactions are, however, more important, and are undoubtedly responsible for the major difference in formation equilibria: the dinuclear ligands show only one complex $[M_2(\mathbf{2})_3]^{2z+}$, while the mononuclear ligands give mixtures $[M(\mathbf{1})_n]^{z+}$, $n = 1-3$. The formation of the dinuclear complexes thus obeys the criteria for a strict self-assembly reaction as defined by Lindsey.[4] The *fac* arrangement of the methylpyridine moieties in the dinuclear complexes results in steric repulsions between methyl groups in the 6-positions; this was found previously for Co^{II},[10] and has now been shown to influence the oxidation potential of Fe^{II} and the magnetic spin state, as has been reported previously for spin-crossover complexes.[34,35]

The dinuclear complexes differ significantly from the mononuclear species in two properties: the oxidation potential of $[Co(\mathbf{1a})_3]^{2+}$ and $[Co_2(\mathbf{2a})_3]^{4+}$ and the spin-crossover transitions of $[Fe(\mathbf{1a})_3]^{2+}$ and $[Fe_2(\mathbf{2a})_3]^{4+}$. Both oxidation of Co^{II} and the transition of Fe^{II} from high spin to low spin require shortening of the metal–nitrogen bonds as a result of removing two electrons from the antibonding e_g^* orbitals. The shortening is 0.15–0.20 Å both for spin crossover[28,33] and for oxidation (Table 2), and therefore similar forces will be exerted by the metal ion upon the ligand strands as a result of these transitions. The complex $[Co_2(\mathbf{2a})_3]^{4+}$ is more readily oxidized than $[Co(\mathbf{1a})_3]^{2+}$, and $[Fe_2(\mathbf{2a})_3]^{4+}$ shows greater stability in the low-spin state than $[Fe(\mathbf{1a})_3]^{2+}$; both observations suggest that the dinuclear system favours the form with the shorter bond lengths.

This is not the only possible explanation: it was suggested on the basis of theoretical calculations[36,37] that spin crossover takes place by means of a trigonal twist, and the degree of trigonal twist has been correlated with the amount of high-spin form present; low values of the twist angle ω correspond to the high-spin state.[35,38] If this is so, then constraints in the helical structure might prevent the untwisting necessary to lead to the high-spin state. As we have discussed elsewhere, Bailar and Rây-Dutt twists are impossible for these triple-helix structures.[16] This restriction of twisting would not, however, be expected to stabilize the Co^{III} oxidation state in $[Co_2(\mathbf{2a})_3]^{6+}$, and so the size-selectivity argument, which explains both effects, seems preferable.

Experimental Section

Materials: Solvents and starting materials were purchased from Fluka AG (Buchs, Switzerland) and used without further purification unless otherwise stated. Ion-exchange column chromatography was performed with Sephadex SP C25 (Sigma) or Dowex 1X2 (Fluka).

Spectroscopic and analytical measurements: UV/Vis spectra were recorded in acetonitrile at 10^{-3} to 10^{-4} M concentration in quartz cells of 1 and 0.1 cm path length in Perkin–Elmer Lambda 5 and Lambda 2 spectrometers. Spectrophotometric titrations were performed as described previously.[14b] Absorbance data were collected at ten different wavelengths, and the number of absorbing species was determined by factor analysis. The data were then fitted to the proposed equilibium model by the procedure described by Gampp et al.[39] The average difference between observed and calculated absorbances was typically 0.003 absorbance units. IR spectra were obtained from KBr pellets in a Perkin–Elmer 883 spectrometer. Cyclic voltammograms were measured on Tacussel PRGE-DEC or BAS-CV-50 W potentiostats linked to a function generator. A three-electrode system was used, with a stationary Pt disc as working electrode, a Pt counterelectrode and a nonaqueous Ag/Ag^+ reference electrode. The inert electrolyte was Bu_4NClO_4 (0.1 M in CH_3CN), previously recrystallized from ethanol. Acetonitrile was freshly distilled over P_2O_5 and passed through an alox I column prior to use. The reference potential was standardized with $[Ru(bipy)_3](ClO_4)_2$.[40] Voltammograms were recorded at 100 mV s^{-1} and analysed according to established procedure.[40] ES-MS spectra were recorded on a Finnigan-Mat SSQ 7000 spectrometer at the Mass Spectroscopy Laboratory of the University of Geneva. ^1H and ^{13}C NMR spectra were recorded on a Varian Gemini 300 spectrometer; chemical shifts are relative to TMS as internal standard; the temperature was calibrated as previously described.[41] Magnetic susceptibilities in CD_3CN were measured by the Evans method[25] on the Varian Gemini 300 spectrometer, with modifications for a superconducting magnet.[42] Data were corrected for diamagnetic contribution of the ligand with the molar susceptibility of **2a** for dinuclear triple helices and half of this value for the mononuclear complexes.[25,43] The apparent molar susceptibility measured for **2a** was -4.44×10^{-4} cm^3 mol^{-1} at 293 K for a concentration of 0.024 M. Molar susceptibilities of the complexes were measured at 10 K intervals between 243 and 333 K. The densities of solutions in acetonitrile d_t were corrected for temperature.[25,44]

Molar susceptibilities were converted to effective magnetic moments μ_{eff} by Equation (10).[19] Elemental analyses were performed at the Microanalytical Laboratory of the University of Geneva. Metal contents were determined by atomic absorption spectroscopy after acidic mineralization.

$$\mu_{eff} = 2.828\sqrt{\frac{T.MW}{S_f.c}\left(\frac{\Delta\upsilon}{\upsilon} + S_f.c.\chi_0 - \frac{S_f.c}{MW}\chi_d\right)} \qquad (10)$$

Preparation of the ligands: The ligands 5-methyl-2-(1-methylbenzimidazol-2-yl)pyridine (**1a**),[16] 6-methyl-2-(1-methylbenzimidazol-2-yl)pyridine (**1b**),[14b] bis[5-(1-methyl-2-(5′-methyl-2′-pyridyl)benzimidazolyl)]methane (**2a**),[16] bis[5-(1-methyl-2-(6′-methyl-2′-pyridyl)benzimidazolyl)]methane (**2b**),[14] and bis[5-(1-ethyl-2-(5′-methyl-2′-pyridyl)benzimidazolyl)]methane (**2c**)[16] were prepared according to literature procedures.

Preparation of the complexes: **Caution!** Combinations of perchlorate salts with organic solvents are potentially explosive and should be handled with the necessary care.[45] The complexes $[Co(\mathbf{1a})_3](ClO_4)_2 \cdot MeOH$[16] and $[Co_2(\mathbf{2a})_3](ClO_4)_4$[14] were prepared according to literature procedures.

$[Fe(\mathbf{1a})_3](ClO_4)_2$: Compound **1a** (67 mg, 0.031 mmol) was dissolved in CH_2Cl_2 (2 mL), and $Fe(ClO_4)_2 \cdot 6H_2O$ (36.3 mg, 0.1 mmol) in acetonitrile (8 mL) was added. The violet solution was evaporated to dryness, the solid was dissolved in acetonitrile (2 mL) and ether was added to the solution until precipitation began. The mixture was cooled (-20 °C) and the violet solid collected by filtration to give 92.4 mg (96%) of $[Fe(\mathbf{1a})_3](ClO_4)_2 \cdot 2H_2O$. $FeC_{42}H_{39}N_9Cl_2O_8 \cdot 2H_2O$: calcd C 52.50, H 4.52, N 13.12; found C 52.50, H 4.34, N 12.80; IR: $\tilde{\nu}$ = 3119, 3063 [ν(CHAr)]; 1602, 1584 [ν(C=C), ν(C=N)]; 1473, 1442 [$\delta(CH_3)$]; 1090, 622 cm^{-1} [$\nu(ClO_4)$]; UV/Vis (acetonitrile): λ_{max} (ε) = 332 (63060), 520 nm (4530); ES-MS (CH_3CN): m/z = 362.8 ($[Fe(\mathbf{1a})_3]^{2+}$, 100%), 224.1 ($[\mathbf{1a}+H]^+$, 20%).

$[Fe(\mathbf{1b})_3](ClO_4)_2$: The complex was obtained similarly to $[Fe(\mathbf{1a})_3](ClO_4)_2$ from $Fe(ClO_4)_2 \cdot 6H_2O$ (61 mg, 0.168 mmol) and **1b** (112.4 mg, 0.050 mmol). After drying (6 h/10^{-2} Torr/50 °C), 122 mg (77%) of $[Fe(\mathbf{1b})_3](ClO_4)_2 \cdot H_2O$ was obtained as a yellow solid. $FeC_{42}H_{39}N_9Cl_2O_8 \cdot H_2O$: calcd C 53.51, H 4.39, N 13.38; found C 53.11, H 4.22, N 13.30; IR:

$\tilde{\nu}$ = 3074 [ν(CHAr)]; 1603, 1570 [ν(C=C), ν(C=N)]; 1483, 1438 [δ(CH_3)]; 1089, 622 cm^{-1} [ν(ClO_4)]; UV/Vis (acetonitrile): λ_{max} (ε) = 310 (57050), 385 (sh) nm (972); ES-MS (CH_3CN): m/z = 362.8 ([Fe(**1b**)$_3$]$^{2+}$, 100%), 271.6 ([Fe(**1b**)$_2$(CH_3CN)]$^{2+}$, 41%), 224.1 ([**1b**+H]$^+$, 20%).

[Fe$_2$(2a)$_3$](ClO$_4$)$_4$: Compound **2a** (100 mg, 0.218 mmol) in CH_2Cl_2 (1 mL) was added to $Fe(ClO_4)_2 \cdot 6H_2O$ (53 mg, 0.146 mmol) in acetonitrile (5 mL). The solution, which immediately turned deep violet, was evaporated to dryness, the solid was dissolved in acetonitrile (1 mL), and methanol was slowly diffused into the solution. After filtration and drying (2 h/10^{-2} Torr/20 °C), 120.6 mg (84%) of deep violet crystals were obtained. $Fe_2C_{87}H_{78}N_{18}Cl_4O_{16} \cdot 2H_2O \cdot CH_3CN$: calcd C 54.46, H 4.37, N 13.56; found C 54.33, H 4.70, N 13.34; UV/Vis (acetonitrile): λ_{max} (ε) = 332 (141000), 534 nm (12800); ^{1}H NMR (300 MHz, CD_3CN, 25 °C, TMS): δ = 2.04 (s, 18H), 3.42 (s, 6H), 3.67 (s, 6H), 4.95 (s, 18H), 6.85 (d, 6H), 7.59 (d, 6H), 8.34 (d, 6H), 9.61 (s, br, 6H), 10.44 (d, 6H); ^{13}C NMR (75.44 MHz, CD_3CN, 25 °C): δ = 20.8, 37.5 (CH_3); 40.9 (CH_2); 117.3, 117.8, 127.5, 132.6, 140.9, 157.3 (CH); 137.7, 138.1, 147.3, 152.7, 166.5 (br), 163.5 (br, C_{quat}).

[Fe$_2$(2b)$_3$](ClO$_4$)$_4$: $Fe(ClO_4)_2 \cdot 6H_2O$ (50.0 mg, 0.137 mmol) in acetonitrile (1 mL) was added to **2b** (95 mg, 0.207 mmol) in CH_2Cl_2 (2 mL). The deep yellow solution was stirred for 5 min and evaporated to dryness. The solid was dissolved in the minimum amount of acetonitrile, and precipitation was achieved by addition of diethyl ether to the concentrated solution and cooling the mixture to −20 °C to give 124 mg (93%) of $[Fe_2(\mathbf{2b})_3](ClO_4)_4 \cdot 4H_2O$ as a yellow powder. $Fe_2C_{87}H_{78}N_{18}Cl_4O_{16} \cdot 4H_2O$: calcd C 53.38, H 4.43, N 12.88; found C 53.29, H 4.40, N 12.87; IR: $\tilde{\nu}$ = 3079 [ν(CHAr)]; 1604, 1570 [ν(C=C), ν(C=N)]; 1486, 1431 [δ(CH_3)]; 1091, 622 cm^{-1} [ν(ClO_4)]; UV/Vis (acetonitrile): λ_{max} (ε) = 320 nm (94280); ES-MS (CH_3CN): m/z = 371.7 ([Fe$_2$(**2b**)$_3$]$^{4+}$, 100%), 271.6 ([Fe$_2$(**2b**)$_3$](ClO_4)]$^{3+}$, 8%), 459.6 ([**2b**+H]$^+$, <5%).

[Fe$_2$(2c)$_3$](ClO$_4$)$_4$: The complex was obtained similarly to $[Fe_2(\mathbf{2a})_3](ClO_4)_4$ from $Fe(ClO_4)_2 \cdot 6H_2O$ (19.2 mg, 0.053 mmol) and **2c** (38.6 mg, 0.079 mmol) to give deep violet crystals of $[Fe_2(\mathbf{2c})_3](ClO_4)_4 \cdot 4.6H_2O$ (43 mg, 79%). Slow diffusion of methanol into a concentrated solution of the complex in CH_3CN gave crystals suitable for X-ray diffraction. $Fe_2C_{93}H_{90}N_{18}Cl_4O_{16} \cdot 4.6H_2O$: calcd C 54.41, H 4.88, N 12.28; found C 54.59, H 5.01, N 12.21; ^{1}H NMR (300 MHz, CD_3CN, 25 °C, TMS): δ = 1.81 (t, ^3J = 6.6 Hz), 2.05 (s, 18H), 3.38 (s, 6H), 3.90 (s, 6H), 5.25 (m, 12H), 6.85 (d, 6H), 7.61 (d, 6H), 8.33 (d, 6H), 9.62 (br s, 6H), 10.24 (d, 6H); ^{13}C NMR (75.44 MHz, CD_3CN, 25 °C): δ = 16.9, 21.6 (CH_3); 41.2 (CH_2); 117.6, 117.8, 128.1, 133.6, 141.7, 156.9 (CH); 136.2, 137.4, 146.7, 155.0, 158.5, 165.8 (C_{quat}); IR: $\tilde{\nu}$ = 1604, 1570 (C=C, C=N), 1091, 622 cm^{-1} (ClO_4); UV/Vis (acetonitrile): λ_{max} (ε) = 332 (134000), 532 nm (12650); ES/MS (CH_3CN): m/z = 393.4 [Fe$_2$(**2c**)$_3$]$^{4+}$, 556.8 [Fe$_2$(**2c**)$_3$(ClO_4)]$^{3+}$, 885.2 [Fe$_2$(**2c**)$_3$(ClO_4)$_2$]$^{2+}$.

[Co(1a)$_3$](ClO$_4$)$_3$: $[Co(\mathbf{1a})_3](ClO_4)_2 \cdot MeOH$ (413 mg, 0.49 mmol) was dissolved in acetonitrile (10 mL) and H_2O_2 (100 μL, 30% in water) and $HClO_4$ (130 μL, 70% in water) were added together with $[Cp_2Fe]BF_4$ (2 mg) The solution was heated for 14 h at 40 °C. After cooling, the solution was concentrated under reduced pressure and the complex precipitated by adding a saturated solution of $LiClO_4$ in water. The red-orange solid was collected by filtration, washed with cold water, dissolved in 5 mL of acetonitrile and diluted to 100 mL with water. The complex was absorbed on Dowex 50WX2 cation exchange resin in the H^+ form (10 g). The resin was placed on a column of the same resin (diameter 1 cm, length 50 cm). Elution with increasing concentration of aqueous HCl (1–4 M) gave two distinct bands corresponding to the two isomers; the *mer* isomer was eluted first. Fractions of the *mer* isomer were collected, evaporated to dryness and dissolved in the minimum amount of MeOH. The insoluble residue was filtered off and the complex precipitated by addition of THF. Recrystallization from methanol/acetone gave 98 mg (24%) of orange *mer*-[Co(**1a**)$_3$]Cl_3. ^{1}H NMR (300 MHz, CD_3OD, 25 °C, TMS): δ = 2.37 (s, 3H), 2.40 (s, 3H), 2.48 (s, 3H), 4.41 (s, 3H), 4.44 (s, 3H), 4.65 (s, 3H), 5.23 (d, 1H, ^3J = 7.7 Hz), 5.31 (d, 1H, ^3J = 7.7 Hz), 5.46 (d, 1H, ^3J = 7.6 Hz), 7.03 (t, 1H, ^3J = 7.6 Hz), 7.23 (dt, 1H, ^3J = 7.3 Hz, $^4J \leq 1$ Hz), 7.29 (t, 1H, ^3J = 8.0 Hz), 7.52 (t, 1H, ^3J = 7.9 Hz), 7.55 (s, 1H), 7.56 (t, 1H, ^3J = 9.1 Hz), 7.63 (t, 1H, ^3J = 8.0 Hz), 7.75 (s, 1H), 7.77 (s, 1H), 7.91 (d, 1H, ^3J = 8.4 Hz), 7.97 (d, 1H, ^3J = 8.0 Hz), 7.99 (d, 1H, ^3J = 8.5 Hz), 8.45 (d, 1H, ^3J = 7.9 Hz), 8.46 (d, 1H, ^3J = 8.3 Hz), 8.54 (d, 1H, ^3J = 8.2 Hz), 8.73 (d, 1H, ^3J = 8.4 Hz), 8.86 (d, 1H, ^3J = 8.2 Hz), 8.89 (d, 1H, ^3J = 8.4 Hz); ^{13}C NMR (75.44 MHz, CD_3OD, 25 °C): δ = 19.24, 19.42, 19.50, 34.25, 34.35, 34.39 (CH_3), 114.72, 114.74, 114.80, 114.99, 115.02, 115.43, 127.98, 128.16, 128.25, 128.45, 128.46, 128.72, 128.81, 128.98, 129.27, 145.23, 145.78, 146.01, 154.90, 155.00, 155.37 (CH), 137.66, 138.02, 138.51, 139.06, 139.19, 139.22, 144.00, 144.43, 144.46, 146.06, 146.52, 147.45, 152.11, 152.70, 152.75 (C_{quat}); IR: $\tilde{\nu}$ = 3040 [ν(CHAr)]; 1606, 1583, 1550 [ν(C=C), ν(C=N)]; 1481, 1416 [δ_{asym}(CH_3)], 831, 743 [δ(CHAr)]; UV/Vis (acetonitrile): λ_{max} (ε) = 338 nm (38700).

Fractions of the *fac* isomer were collected, evaporated to dryness, dissolved in 5 mL of water and precipitated with saturated $NaClO_4$ in water. Slow diffusion of *tert*-butyl methyl ether into a concentrated solution of fac-[Co(**1a**)$_3$](ClO_4)$_3$ in propionitrile afforded red prisms suitable for X-ray diffraction. Yield: 37 mg (6%) $CoC_{42}H_{39}N_9Cl_3O_{12} \cdot C_2H_5CN$: calcd C 49.93, N 12.94, H 4.11; found C 49.68, N 12.84, H 4.13; ^{1}H NMR (300 MHz, CD_3CN, 25 °C, TMS): δ = 2.37 (s, 3H), 4.44 (s, 3H), 5.24 (d, 1H, ^3J = 8.6 Hz), 7.07 (m, 1H), 7.20 (s, 1H), 7.55 (m, 1H), 7.89 (d, 1H, ^3J = 8.5 Hz), 8.25 (d, 1H, ^3J = 8.4 Hz), 8.56 (d, 1H, ^3J = 8.3 Hz); ^{13}C NMR (75.44 MHz, CD_3CN, 25 °C): δ = 19.70, 34.92 (CH_3), 114.87, 115.08, 127.73, 128.11, 128.54, 144.51, 154.64 (CH), 138.10, 139.14, 144.24, 144.80, 151.71 (C_{quat}); IR: $\tilde{\nu}$ = 3123 [ν(CHAr)], 2242 [ν(C=C)], 1605, 1585, 1545 [ν(C=C), ν(C=N)], 1482 [δ(CH_3)], 1089, 621 [ν(ClO_4)]; UV/Vis (acetonitrile): λ_{max} (ε) = 334 (44000), 521(sh) nm (180).

Crystal structure of *fac*-[Co(1a)$_3$](ClO$_4$)$_3$·EtCN: $Co(C_{14}H_{13}N_3)_3(C_3H_5N)(ClO_4)_3$, M_r = 1082.2, $F(000)$ = 1116. Red prism, 0.076 × 0.24 × 0.24 mm, mounted on a quartz fibre with RS3000®. Triclinic, $P\bar{1}$, Z = 2, a = 11.201(1), b = 13.487(1), c = 17.434(1) Å, α = 84.657(4)°, β = 80.094(4)°, γ = 65.895(5)°, V = 2367.4(4) Å^3, from 23 reflections (37 < 2θ < 62°), ρ_{calcd} = 1.52 g cm^{-3}. Cell dimensions and intensities were measured at 170 K on a Nonius CAD4 diffractometer with $Cu_{K\alpha}$ radiation (λ = 1.5418 Å), ω − 2θ scan; two reference reflections measured every 45 min showed variations less than 3.0$\sigma(I)$. (4 < 2θ < 110°); 5930 measured reflections, of which 5019 were observable ($|F_o| > 4\sigma(F_o)$). Data were corrected for anomalous dispersion, Lorentzian polarization and absorption effects (μ = 5.033 mm^{-1}, absorption coefficient A^*, min 1.471, A^* max 2.938).[46] Solution by direct methods with MULTAN 87,[47] all other calculations used the XTAL 3.2[48] system and ORTEP II[49] programs. The 21 aromatic hydrogen atoms were refined isotropically; non-hydrogen atoms were refined anisotropically with atomic scattering factors and anomalous dispersion terms taken from ref. [50]. Full-matrix least-squares refinement on $|F|$ with weights of $1/\sigma^2(F_o)$ gave final values of R = 0.079, R_w = 0.054 for 704 variables and 5019 contributing reflections. The mean shift/error on the last cycle was 0.0027, and the maximum was 0.078. The final difference electron density map showed maximum and minimum of +1.20 and −0.87 e Å^{-3}.

Crystal structure of [Fe$_2$(2c)$_3$](ClO$_4$)$_4$·4CH$_3$CN: $Fe_2(C_{31}H_{30}N_6)_3(ClO_4)_4(CH_3CN)_4$, M_r = 2133.6, $F(000)$ = 4440. Violet prism, 0.20 × 0.25 × 0.25 mm, mounted in a capillary containing mother liquor. Monoclinic, $C2/c$, Z = 4, a = 27.193(6), b = 15.477(5), c = 24.814(3) Å, β = 96.00(2)°, V = 10386(4) Å^3, from 28 reflections (11 < 2θ < 23°), ρ_{calcd} = 1.36 g cm^{-3}. Cell dimensions and intensities measured at room temperature on a Stoe STAD14 diffractometer with $Mo_{K\alpha}$ radiation (λ = 0.71069 Å), ω–2θ scan, two reference reflections measured every 60 min showed variations of about 7% during data collection, and data were corrected for this drift. 10019 measured reflections, 3 < 2θ < 40°, 4849 unique reflections, 2809 observable ($|F_o| > 4\sigma(F_o)$); R_{int} = 0.082 for equivalent reflections. Data were corrected for anomalous dispersion and Lorentzian polarization, but not absorption (μ = 0.454 mm^{-1}).[46] Solution by direct methods and other calculations as above. Non-hydrogen atoms of the cation and one perchlorate refined anisotropically, other atoms isotropically and hydrogen atoms in calculated positions. Full-matrix least-squares refinement on $|F|$ with unit weights gave final values of R = 0.082, R_w = 0.082 for 658 variables and 2785 contributing reflections. The mean shift/error on the last cycle was 0.012, and the maximum was 0.38. The final difference electron density map showed a maximum and minimum of +0.72 and −0.78 e Å^{-3}. The cation lies on a twofold axis passing through C13a. One perchlorate is perfectly ordered (refined with anisotropic displacement parameters for Cl and O), the second is totally disordered (two sites for Cl). Four acetonitrile molecules were found, essentially located in large interstices between helices. One methyl group of the ethyl substituents is disordered and was refined on two sites with population parameters of 0.5.

Crystallographic data (excluding structure factors) for the structures reported in this paper have been deposited with the Cambridge Crystallographic Data Centre as supplementary publication no. CCDC-100318. Copies of the data can be obtained free of charge on application to CCDC,

0947-6539/98/0403-0492 $ 17.50+.50/0 *Chem. Eur. J.* **1998**, *4*, No. 3

12 Union Road, Cambridge CB2 1EZ, UK (fax: (+ 44) 1223-336-033; e-mail: deposit@ccdc.cam.ac.uk).

Acknowledgements: We thank Werner Kloeti for recording ESMS spectra. This research is supported by the Swiss National Science Foundation.

Received: May 9, 1997 [F689]

[1] A. F. Williams, *Chem. Eur. J.* **1997**, *3*, 15.
[2] E. C. Constable in *Comprehensive Supramolecular Chemistry, Vol. 6* (Eds.: J. L. Atwood, J. E. D. Davies, D. D. MacNicol, F. Vögtle, J.-M. Lehn), Pergamon, Oxford, **1996**, p. 213.
[3] C. Piguet, G. Bernardinelli, G. Hopfgartner, *Chem. Rev.* **1997**, *97*, 2005.
[4] J. S. Lindsey, *New J. Chem.* **1991**, *15*, 153.
[5] J.-M. Lehn, *Supramolecular Chemistry*, Wiley, Chichester, **1995**; J.-M. Lehn, *Angew. Chem.* **1988**, *100*, 91; *Angew. Chem. Int. Ed. Engl.* **1988**, *27*, 89.
[6] J. Libman, Y. Tor, A. Shanzer, *J. Am. Chem. Soc.* **1987**, *109*, 5880.
[7] R. Krämer, J.-M. Lehn, A. De Cian, J. Fischer, *Angew. Chem. Int. Ed. Engl.* **1993**, *32*, 703; *Angew. Chem.* **1993**, *105*, 764.
[8] L. J. Charbonnière, G. Bernardinelli, C. Piguet, A. M. Sargeson, A. F. Williams, *J. Chem. Soc. Chem. Commun.* **1994**, 1419.
[9] a) S. Ferrere, C. M. Elliott, *Inorg. Chem.* **1995**, *34*, 5818; b) B. R. Serr, K. A. Andersen, C. M. Elliott, O. P. Anderson, *ibid.* **1988**, *27*, 4499; c) C. M. Elliott, D. L. Derr, S. Ferrere, M. D. Newton, Y.-P. Liu, *J. Am. Chem. Soc.* **1996**, *118*, 5221; d) S. L. Larson, S. M. Hendrikson, S. Ferrere, D. L. Derr, C. M. Elliott, *ibid.* **1995**, *117*, 5881.
[10] C. Piguet, G. Bernardinelli, B. Bocquet, O. Schaad, A. F. Williams, *Inorg. Chem.* **1994**, *33*, 4112.
[11] K. T. Potts, M. Keshavarz-K, F. S. Tham, H. D. Abruña, C. R. Arana, *Inorg. Chem.* **1993**, *32*, 4422; K. T. Potts, M. Keshavarz-K, F. S. Tham, H. D. Abruña, C. R. Arana, *ibid.* **1993**, *32*, 4436; K. T. Potts, M. Keshavarz-K, F. S. Tham, K. A. Gheysen Raiford, C. R. Arana, H. D. Abruña, *ibid.* **1993**, *32*, 5477.
[12] C. Piguet, J.-C. G. Bünzli, G. Bernardinelli, G. Hopfgartner, A. F. Williams, *J. Am. Chem. Soc.* **1993**, *115*, 8197; C. Piguet, A. F. Williams, G. Bernardinelli, J.-C. G. Bünzli, *Inorg Chem.* **1993**, *32*, 4139; J.-C. G. Bünzli, P. Froidevaux, C. Piguet, *New J. Chem.* **1995**, *19*, 661; C. Piguet, G. Bernardinelli, J.-C. G. Bünzli, S. Petoud, G. Hopfgartner, *J. Chem. Soc. Chem. Commun.* **1995**, 2575; C. Piguet, J.-C. G. Bünzli, G. Bernardinelli, C. G. Bochet, P. Froidevaux, *J. Chem. Soc. Dalton Trans.* **1995**, 83.
[13] C. Piguet, J.-C. G. Bünzli, *Eur. J. Solid-State Chem.* **1996**, *33*, 165.
[14] a) A. F. Williams, C. Piguet, G. Bernardinelli, *Angew. Chem.* **1991**, *103*, 1530; *Angew. Chem. Int. Ed. Engl.* **1991**, *30*, 1490; b) C. Piguet, G. Bernardinelli, B. Bocquet, A. Quattropani, A. F. Williams, *J. Am. Chem. Soc.* **1992**, *114*, 7440.
[15] L. J. Charbonnière, M. F. Gilet, K. Bernauer, A. F. Williams, *Chem. Commun.* **1996**, 39.
[16] L. J. Charbonnière, A. F. Williams, U. Frey, A. E. Merbach, P. Kamalaprija, O. Schaad, *J. Am. Chem. Soc.* **1997**, *119*, 2488.
[17] B. Kersting, J. R. Telford, M. Meyer, K. N. Raymond, *J. Am. Chem. Soc.* **1996**, *118*, 5712; B. Kersting, M. Meyer, R. E. Powers, K. N. Raymond, *ibid.* **1996**, *118*, 7221.
[18] C. Bochet, C. Piguet, A. F. Williams, *Helv. Chim. Acta* **1993**, *76*, 372.
[19] C. Piguet, E. Rivara-Minten, G. Hopfgartner, J.-C. G. Bünzli, *Helv. Chim. Acta.* **1995**, *78*, 1651; C. Piguet, E. Rivara-Minten, G. Bernardinelli, J.-C. G. Bünzli, G. Hopfgartner, *J. Chem. Soc. Dalton Trans.* **1997**, 421.
[20] S. Rüttimann, C. M. Moreau, A. F. Williams, G. Bernardinelli, A. W. Addison, *Polyhedron*, **1992**, *11*, 635.
[21] K. Yanagi, Y. Ohashi, Y. Sasada, Y. Kaizin, H. Kobayashi, *Bull. Chem. Soc. Jpn.* **1981**, *54*, 118.
[22] E. C. Constable, *Tetrahedron* **1992**, *48*, 10013.
[23] A. G. Orpen, L. Brammer, F. H. Allen, O. Kennard, D. G. Watson, R. Taylor, *J. Chem. Soc. Dalton Trans.* **1989**, S1.
[24] D. F. Evans, *J. Chem. Soc.* **1959**, 2003; D. Ostfed, I. A. Cohen, *J. Chem. Educ.* **1972**, *49*, 829.
[25] C. Piguet, *J. Chem. Educ.* **1997**, *74*, 815.
[26] F. A. Cotton, G. Wilkinson, *Advanced Inorganic Chemistry*, 5th ed., Wiley, New York, **1988**.
[27] B. A. Katz, C. E. Strouse, *Inorg. Chem.* **1980**, *19*, 658.
[28] P. Gütlich, A. Hauser, H. Spiering, *Angew. Chem.* **1996**, *106*, 2109; *Angew. Chem. Int. Ed. Engl.* **1996,** *33*, 2024.
[29] D. Onggo, H. A. Goodwin, *Aust. J. Chem.* **1991**, *44*, 1539.
[30] R. A. Marcus, N. Sutin, *Biochim. Biophys. Acta* **1985**, *811*, 265.
[31] R. G. Wilkins, *Kinetics and Mechanism of Reactions of Transition Metal Complexes*, 2nd ed., VCH, Weinheim, **1991**, ch. 5.
[32] D. E. Richardson, H. Taube, *Inorg. Chem.* **1981**, *20*, 1278.
[33] J. K. McCusker, A. L. Rheingold, D. N. Hendrickson, *Inorg. Chem.* **1996**, *35*, 2100.
[34] H. Toftlund, S. Yde-Andersen, *Acta Chem. Scand. A* **1981**, *35*, 575.
[35] L. J. Wilson, D. Georges, M. A. Hoselton, *Inorg. Chem.* **1975**, *14*, 2968.
[36] L. G. Vanquickenborne, K. Pierloot, *Inorg. Chem.* **1981**, *20*, 3673.
[37] K. F. Purcell, *J. Am. Chem. Soc.* **1979**, *101*, 5147.
[38] H. Toftlund, *Coord. Chem. Rev.* **1989**, *94*, 67.
[39] H. Gampp, M. Maeder, C. J. Meyer, A. D. Zuberbühler, *Talanta* **1985**, *32*, 95.
[40] A. J. Bard, L. R. Faulkner, *Electrochemical Methods, Fundamentals and Applications*, Wiley, New York, **1980**.
[41] C. Amman, P. Meier, A. E. Merbach, *J. Magn. Res.* **1982**, *46*, 319.
[42] M. V. Baker, L. D. Field, T. W. Hambley, *Inorg. Chem.* **1988**, *27*, 2872.
[43] W. Linert, M. Konecny, F. Renz, *J. Chem. Soc. Dalton Trans.* **1994**, 1523.
[44] R. F. Brunel, K. V. Bibber, *International Critical Tables*, McGraw Hill, New York, London, **1930**.
[45] W. C. Wolsey, *J. Chem. Educ.* **1978**, *55*, A355.
[46] E. Blanc, D. Schwarzenbach, H. D. Flack, *J. Appl. Cryst.* **1991**, *24*, 1035.
[47] P. Main, S. J. Fiske, S. E. Hull, L. Lessinger, D. Germain, J. P. Declercq, M. M. Woolfson, *MULTAN 87*, Universities of York (England) and Louvaine-La-Neuve (Belgium), **1987**.
[48] S. R. Hall, H. D. Flack, J. M. Stewart, *XTAL 3.2 User's Manual*, Universities of Western Australia, Geneva and Maryland, **1992**.
[49] C. K. Johnson, *ORTEP II*, report ORNL-5138, Oak Ridge National Laboratory, Oak Ridge, TN, **1976**.
[50] *International Tables for X-Ray Crystallography, Vol. IV*, Kynoch, Birmingham, England, **1974**.